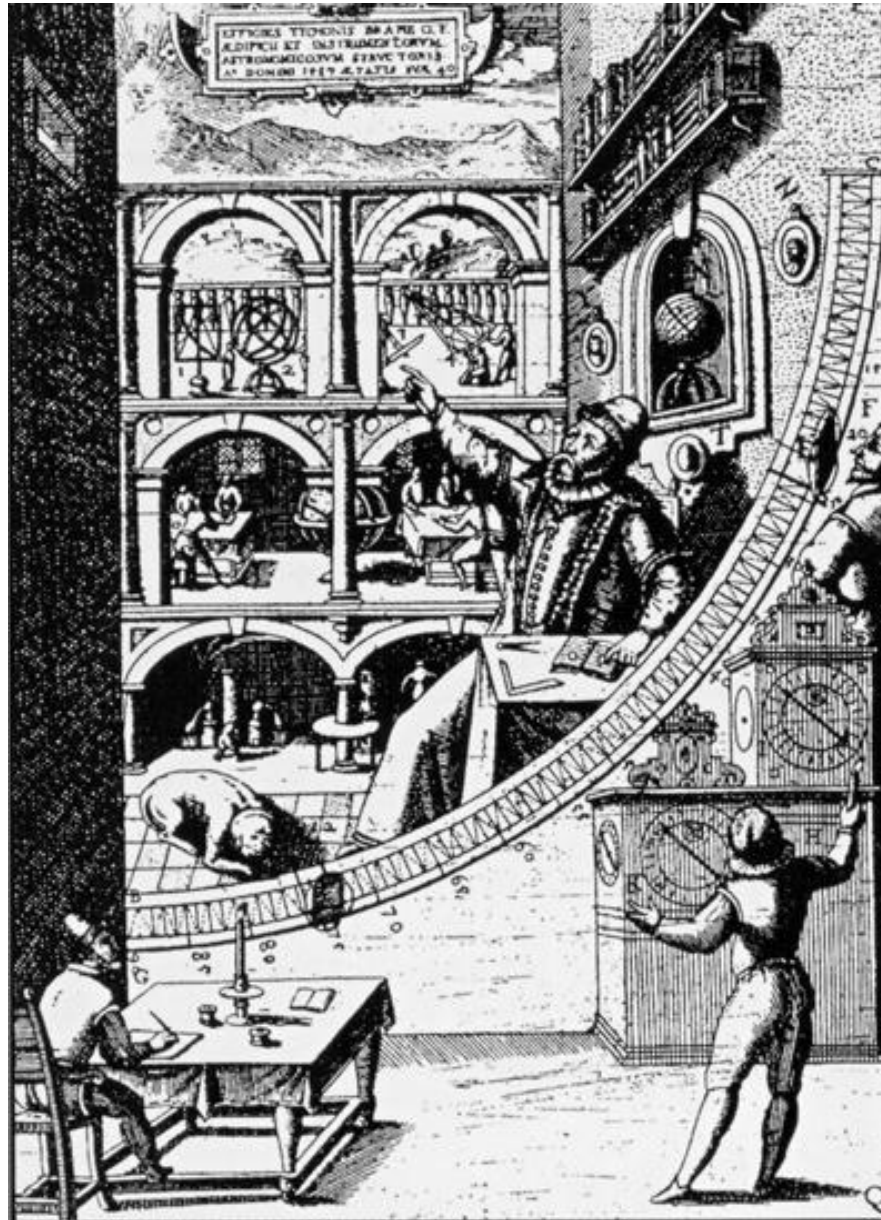


Contents

3	Cosmology for Quasars	97
3.1	The Expanding Universe	97
3.2	Redshift is Expansion	100
3.3	The Hubble Constant is Expansion Speed	102
3.4	Friedman Equations and Cosmological Parameters	103
3.5	The Present Universe is 14 Billion Years Old	111
3.6	Observing Quasars in an Expanding Universe	111
3.6.1	Luminosity Distance and Hubble Diagrams	112
3.6.2	The Angular Width	116
3.6.3	Number Counts	116
3.6.4	The K-Correction	119
3.7	Luminosity Evolution of Quasars	122
3.8	Cosmology with Quasars	123

List of Figures

54	Curvature types	97
55	2dF south galaxy distribution	98
56	COBE hotspots	100
57	Lightcone of observers	101
58	Friedman Evolution	104
59	Cosmic triangle	106
60	CMB data 2002	107
61	Hydra cluster mass distribution	108
62	Elliptical embedded into dark matter	109
63	Fundamental plane of cosmology	110
64	Age as a function of redshift	112
65	Age relations	113
66	Distance modulus as a function of redshift	115
67	Apparent angular width	117
68	Cosmic volume	118
69	SDSS galaxy redshift distribution	120
70	Quasar luminosity evolution with redshift	122
71	Quasar luminosity functions	123



3 Cosmology for Quasars

Quantitative analysis of quasars at redshift $z > 1$ cannot be done without invoking a particular cosmological model. The relativistic Friedmann model is the correct description for the expanding Universe – a Newtonian treatment is completely obsolete. Luminous quasars are now detected up to redshift 6.2; we see these objects, when the Universe was only a few percent of its present age.

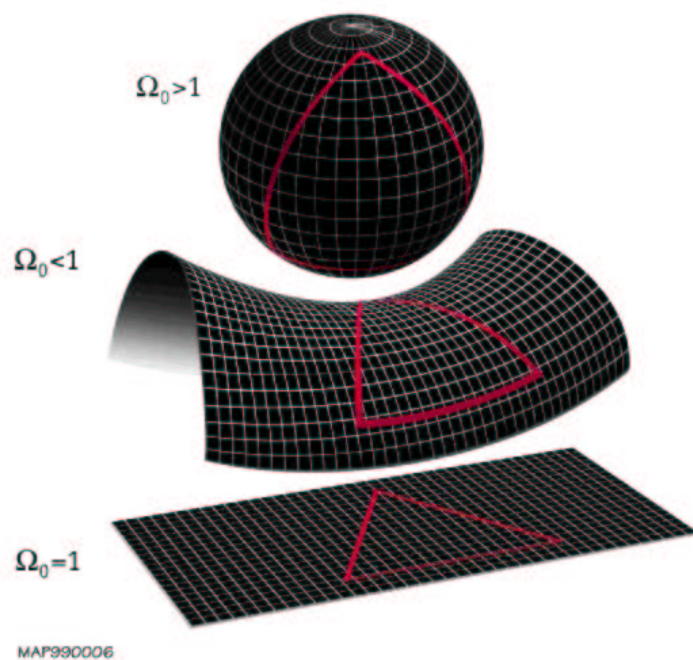


Figure 54: Types of curvature in homogeneous world models.

3.1 The Expanding Universe

According to Einstein's ideas, the Universe is a four-dimensional space-time continuum. One of the key question is therefore how to measure distances and time. In flat space (Minkowski space) this is achieved over the introduction of the metric in Special Relativity

$$ds^2 = c^2 dt^2 - dx^2 - dy^2 - dz^2, \quad (64)$$

which is invariant under Lorentz transformations. This can also be expressed in terms of spherical coordinates

$$ds^2 = c^2 dt^2 - dr^2 - r^2(d\theta^2 + \sin^2 \theta d\phi^2). \quad (65)$$

The paths of freely moving objects through space–time follow the shortest possible paths between two points. For photons, such paths are known as null geodesics given by straight rays on light cones, described by

$$ds^2 = 0. \quad (66)$$

The flat Minkowski space is empty, i.e. it does not contain any form of matter. A

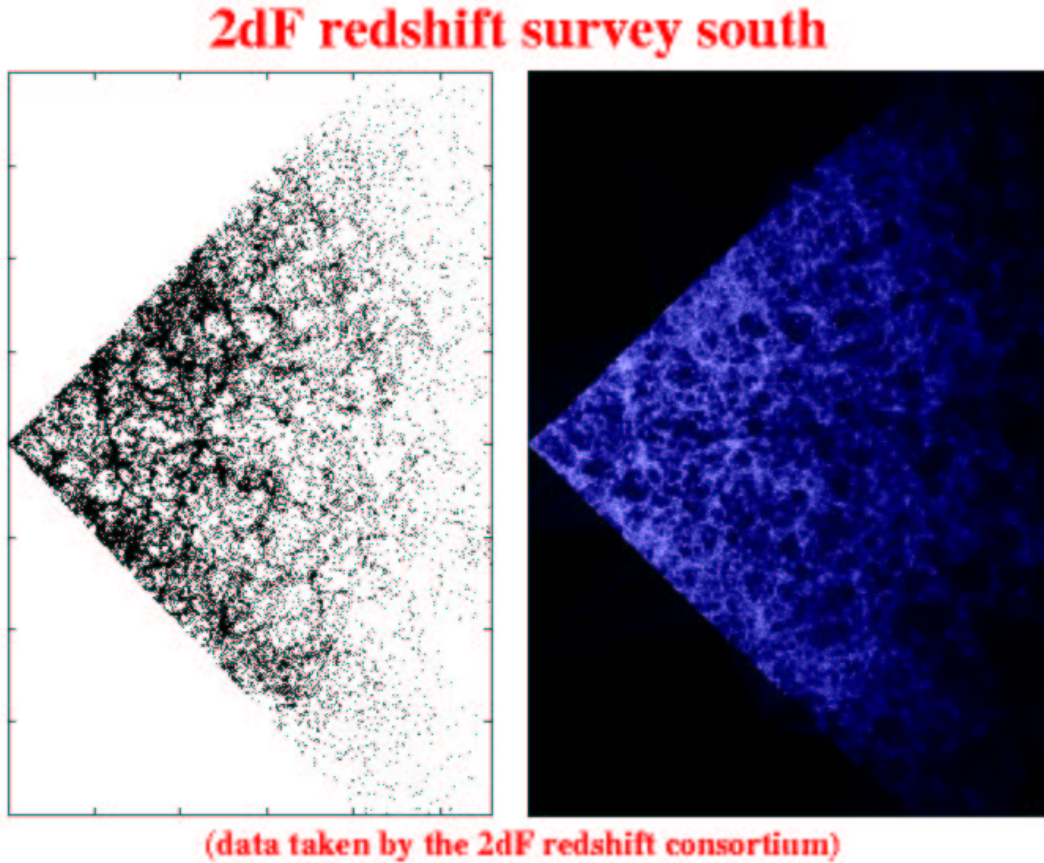


Figure 55: 2dF south galaxy distribution. This proves that the structure on scales of 100 Mpc is uniform. Beyond a redshift of 0.1 only bright galaxies are visible.

universe filled with galaxies, dark matter and photons is, however, curved and no longer flat. In order to constrain the set of all possible such models, one relies on special symmetries:

Homogeneity: It is assumed that the gross properties of the Universe are the same everywhere, if one averages over a suitably large volume. Presently, this means one has to average over scales of 100 Mpc.

Isotropy: It is assumed that the Universe looks approximately the same in every direction for every observer. For our particular location in the Universe, isotropy is fairly well established – the distribution of galaxies is about the same in every direction (except for obscuration along the Milky Way), and the cosmic background radiation (CMB) shows in fact isotropy to a very high accuracy.

The assumption of homogeneity and isotropy is equivalent to a statement that there is nothing special about our location in the Universe. This is known as the **Cosmological Principle**. This is a late realisation of the Copernican principle. On the basis of the above assumptions, mathematicians have derived a more general form of the metric (Robertson 1935; Walker 1936)

$$ds^2 = c^2 dt^2 - R^2(t) \left(\frac{dr^2}{1 - kr^2} + r^2(d\theta^2 + \sin^2 \theta d\phi^2) \right). \quad (67)$$

r , θ and ϕ are now just coordinates taken by a particular observer (a cluster center), and these form a grid which can expand or contract as the size of the Universe changes by the overall scaling factor $R(t)$. These coordinates are referred as comoving coordinates. The expansion parameter $R(t)$ reflects the scale of the Universe as it varies with time. The constant $k = 0, \pm 1$ reflects the sense of curvature of 3-space given by slices $t = \text{const}$: $k = 0$ is flat space; $k = 1$ represents the surface of a three-sphere, and $k = -1$ a negatively curved hyperboloid. The special case of a flat space, $k = 0$, reduces to the above form of the Minkowski metric, except for the presence of the expansion factor which scales all distances in a time-dependent way.

Comoving distances are then measured by a manifold distance

$$d_M = \int_0^r dl = R(t) \int_0^r \frac{dr'}{\sqrt{1 - kr'^2}} = \{R(t) \sin^{-1}(r), R(t)r, R(t) \sinh^{-1}(r)\} \quad (68)$$

for $k = +1, 0, -1$. The measurement of astronomical distances will be discussed later on – distance is not distance ! Similarly, the volume enclosed within a distance from $r = 0$ to r is given by

$$V_k(r) = R^3(t) \int_0^r \int_0^\pi \int_0^{2\pi} \frac{r'^2 dr'}{\sqrt{1 - kr'^2}} \sin \theta d\theta d\phi \quad (69)$$

In flat space, this yields the classical result $V_0(r) = 4\pi R^3(t)r^3/3$, and for $k = \pm 1$

$$V_+(r) = \frac{4\pi}{3} (Rr)^3 \left[\frac{3 \sin^{-1}(r)}{r^3} - \frac{3 \sqrt{1 - r^2}}{r^2} \right] \quad (70)$$

$$V_-(r) = \frac{4\pi}{3} (Rr)^3 \left[-\frac{3 \sinh^{-1}(r)}{r^3} + \frac{3 \sqrt{1 + r^2}}{r^2} \right]. \quad (71)$$

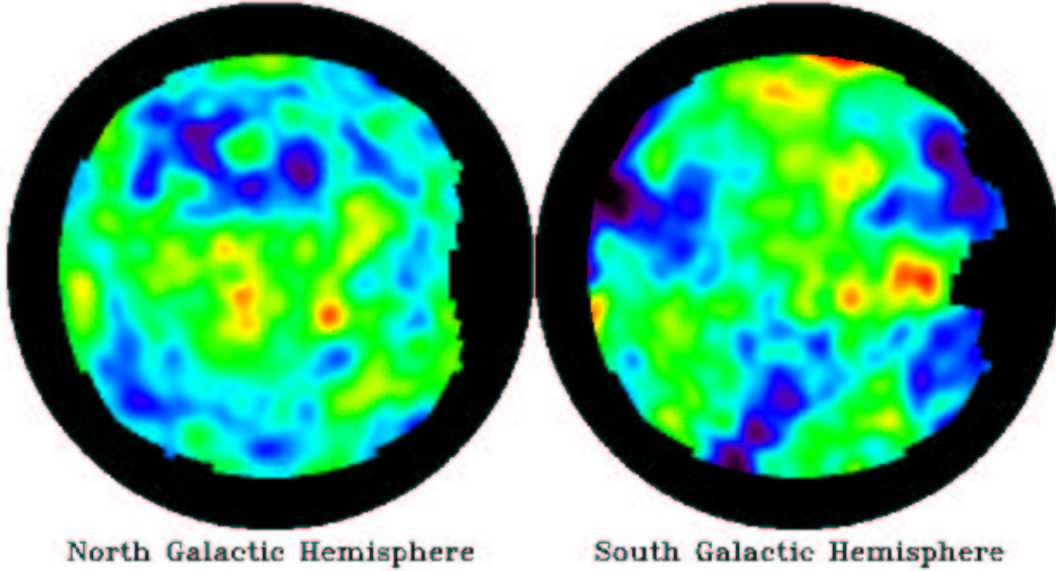


Figure 56: These are two images of the sky (looking north and south of the galactic plane), showing hot spots and cold spots in the cosmic microwave background. The images are based on data taken by the Cosmic Background Explorer satellite. The fluctuations in temperature from the hottest to the coldest regions amount to only one part in 100,000.

The curvature will change slightly the enclosed volumes at large distances with respect to the volume of flat spaces.¹

3.2 Redshift is Expansion

The expansion of the Universe accounts for the redshift of galaxies and quasars. In a contracting Universe, we would observe a blue shift from all objects. Each quasar is given by the coordinates (r, θ, ϕ) . Let us consider a particular quasar Q_1 with position (r_1, θ, ϕ) , emitting light at time t_1 . Photons follow null geodesics, $ds^2 = 0$, where θ and ϕ can be considered as constant (Fig. 57). Therefore

$$c dt = \pm \frac{R dr}{\sqrt{1 - kr^2}}. \quad (72)$$

Since r decreases for light coming towards us, the minus sign is appropriate, the observer is located at $(0, \theta, \phi)$. These photons are now detected at time t_0 requiring

$$\int_{t_1}^{t_0} \frac{c dt}{R(t)} = \int_0^{r_1} \frac{dr}{\sqrt{1 - kr^2}}. \quad (73)$$

¹For small distances $r \ll 1$, the deviation can be evaluated by means of Taylor expansion.

We now consider two waves, emitted at t_1 and $t_1 + \Delta t_1$,

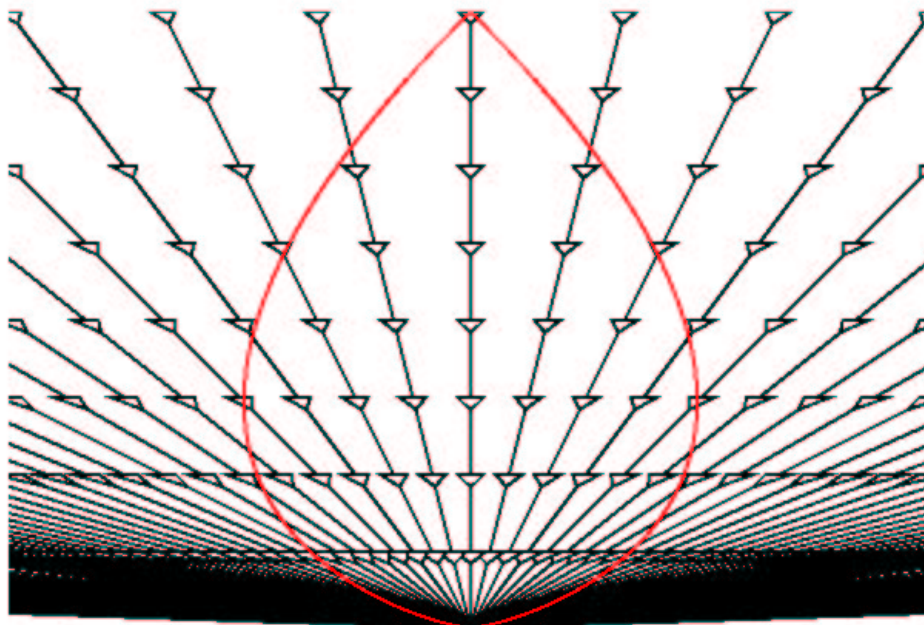


Figure 57: Worldlines of an observer B and of quasars Q in an expanding cosmos. The backward lightcone is still flat in the local Universe, will however be curved in the early Universe. Photons detected by CCDs move along the backward lightcone and are emitted at the intersections with the trajectories of the quasars.

$$\int_{t_1+\Delta t_1}^{t_0+\Delta t_0} \frac{c dt}{R(t)} = \int_0^{r_1} \frac{dr}{\sqrt{1-kr^2}}. \quad (74)$$

If $R(t)$ does not alter drastically in the interval Δt_0 , we obtain by subtracting the two equations

$$\frac{c \Delta t_0}{R(t_0)} - \frac{c \Delta t_1}{R(t_1)} = 0, \quad (75)$$

and therefore

$$\boxed{\frac{c \Delta t_0}{c \Delta t_1} = \frac{\nu_1}{\nu_0} = \frac{\lambda_0}{\lambda_1} = \frac{R(t_0)}{R(t_1)} = 1 + z,} \quad (76)$$

where z denotes the redshift, $z = (\lambda_0 - \lambda_1)/\lambda_1$. **The wavelength of photons is stretched by the expansion of the Universe**, provided $R(t_0) > R(t_1)$. This is the explanation of the redshift of galaxies detected by Hubble.

3.3 The Hubble Constant is Expansion Speed

Though the Hubble constant has been introduced in a completely phenomenological way, it has deep root in the expanding Universe, which is independent on the exact nature of the expansion. It is not a consequence of the Friedman equation.

In order to get the Hubble-law, we expand the metric for small distances r_1

$$\int_0^{r_1} \frac{dr}{\sqrt{1-kr^2}} \simeq r_1, \quad (77)$$

as well as

$$\int_{t_1}^{t_0} \frac{c dt}{R(t)} \simeq \frac{c(t_0 - t_1)}{R(t_0)}. \quad (78)$$

In addition, we use the Taylor-expansion for the expansion factor

$$R(t_1) \simeq R(t_0) - (t_0 - t_1) \left(\frac{\dot{R}}{R} \right)_0 R(t_0) \quad (79)$$

and from redshift

$$R(t_1) = \frac{R(t_0)}{1+z} \simeq R(t_0)(1-z) \quad , \quad z \ll 1. \quad (80)$$

This provides

$$z \simeq (t_0 - t_1) \left(\frac{\dot{R}}{R} \right)_0. \quad (81)$$

From this we get the true distance D_1 of a quasar

$$D_1 = r_1 R(t_0) \simeq c(t_0 - t_1) \simeq \left(\frac{\dot{R}}{R} \right)_0^{-1} cz, \quad (82)$$

also given in the form of the **Hubble-law**

$$\boxed{cz = H_0 D_1.} \quad (83)$$

The constant H_0 , which is defined as

$$\boxed{H_0 = \left(\frac{\dot{R}}{R} \right)_0} \quad (84)$$

is known as the Hubble-constant. Physically, the Hubble-constant is the present expansion speed of the Universe. In a de Sitter Universe, $R(t) \propto \exp(H_0 t)$ it is in fact a true constant. The Hubble-law is a good approximation for redshifts $z < 0.1$.

The Hubble–constant in 2002:

- HST–project (W. Freedman et al. 2001): $H_0 = (72 \pm 8)$ km/s/Mpc;
- Calibration SN Ia (Riess et al. 1996): $H_0 = (65 \pm 7)$ km/s/Mpc.

3.4 Friedman Equations and Cosmological Parameters

The expansion factor $R(t)$ is determined by the Friedman equation (Friedman 1922), $H = \dot{R}/R$,

$$H^2 = \frac{8\pi G}{3} \rho - \frac{kc^2}{R^2} + \frac{c^2 \Lambda}{3} \quad (85)$$

The matter density ρ scales as $\rho = \rho_0(R_0/R)^3$ due to mass conservation. In the radiation dominated era we find $\rho = \rho_0(R_0/R)^4$. Λ denotes the cosmological constant, which is equivalent to a constant vacuum energy density

$$\rho_V = \frac{c^2 \Lambda}{8\pi G} \quad (86)$$

with a corresponding negative pressure $P_V = -\rho_V c^2$. The required value of vacuum energy $\rho_V \simeq \rho_{crit} = 10^{-28}$ g cm $^{-3} \simeq (10^{-4}$ eV) 4 can however not be explained within known theories

$$\rho_V^{QCD} c^2 = (0.3 \text{ GeV})^4 = 1.6 \times 10^{36} \text{ erg/cm}^3 \quad (87)$$

$$\rho_V^{Planck} c^2 = (10^{18} \text{ GeV})^4 = 2 \times 10^{110} \text{ erg/cm}^3. \quad (88)$$

A vacuum energy density always creates repulsive forces, so that the late phase of such a Universe, when the density has decayed, is dominated by vacuum energy with an exponential expansion law, $R(t) \propto \exp(H_\Lambda t)$ (Fig. 58). In High Energy Physics, nowadays more general vacua are discussed given by an equation of state $P_V = w \rho_V$ with $-1 \leq w < -1/3$ (socalled **Quintessence** models).

The present Universe is determined by the Hubble constant $H_0 = (68 \pm 10)$ km/Mpc/sec and the three dimensionless density parameters

- **Matter density parameter:**

$$\Omega_M \equiv \frac{8\pi G}{3H_0^2} \rho_{M,0} = \frac{\rho_{M,0}}{\rho_{crit}} \quad (89)$$

- **Vacuum energy parameter:**

$$\Omega_\Lambda = \frac{\Lambda c^2}{3H_0^2} \quad (90)$$

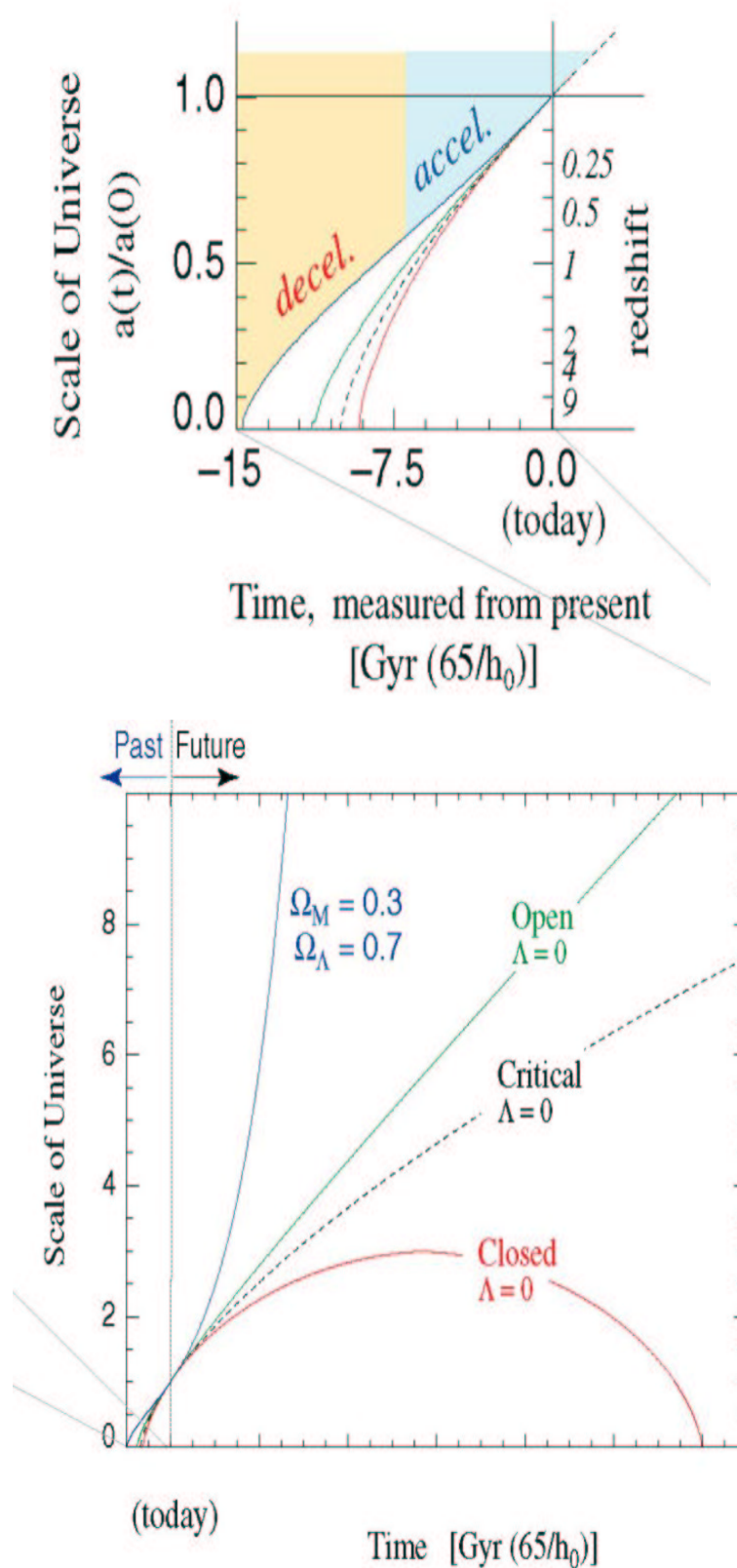


Figure 58: Evolution of cosmological models including a nonvanishing vacuum energy. Time is scaled by the Hubble-constant, taken here as $H_0 = 65$ km/Mpc/sec. The top panel shows the transition from a decelerating Universe towards an accelerating late phase. The transition occurs around a redshift of one. In the lower panel

- **Curvature parameter:**

$$\Omega_k = -\frac{kc^2}{R_0^2 H_0^2} \quad (91)$$

On behalf of the Friedman equation we find

$$\Omega_{\text{tot}} = \Omega_M + \Omega_\Lambda + \Omega_k = 1, \quad (92)$$

or

$$\Omega_k = 1 - \Omega_M - \Omega_\Lambda. \quad (93)$$

The time–evolution of the scale–factor is shown in Fig. 58 for various cosmological parameters. In this respect, it is useful to write the Friedman equation for the normalized expansion factor $a(t) \equiv R(t)/R_0 = 1/(1+z)$

$$\boxed{\frac{da}{dt} = H_0 \sqrt{\frac{\Omega_M}{a} + \Omega_\Lambda a^2 + 1 - \Omega_M - \Omega_\Lambda}.} \quad (94)$$

This can easily be integrated numerically for given parameters H_0 , Ω_M and Ω_Λ . Please, note that there is a second equation following from Einstein's equations

$$2\frac{\ddot{R}}{R} + \frac{\dot{R}^2 + kc^2}{R^2} - c^2\Lambda = -\frac{8\pi GP}{c^2}. \quad (95)$$

This can be reduced to the following form by using the first Friedman equation

$$\frac{\ddot{R}}{R} = -\frac{4\pi G(\rho c^2 + 3P)}{3c^2} + \frac{c^2\Lambda}{3}. \quad (96)$$

This implies $\ddot{R} < 0$ for $\Lambda = 0$, and $\ddot{R} > 0$, whenever vacuum energy is dominant, i.e. a Universe with vacuum energy will accelerate and no longer decelerate.² In Cosmology, also the acceleration parameter q_0 is used

$$q_0 = -\frac{\ddot{R}}{H_0^2 R_0}. \quad (97)$$

There is abundant evidence for the dominance of dark matter and dark energy on the largest distance scales.

- The baryon content of the Universe is constrained by the primordial nucleosynthesis.
- The first information about the large-scale geometry of the Universe for redshifts $z \leq 1$ is provided by data on high- z supernovae, which constrain a combination of the matter density Ω_M and the vacuum energy density Ω_Λ .

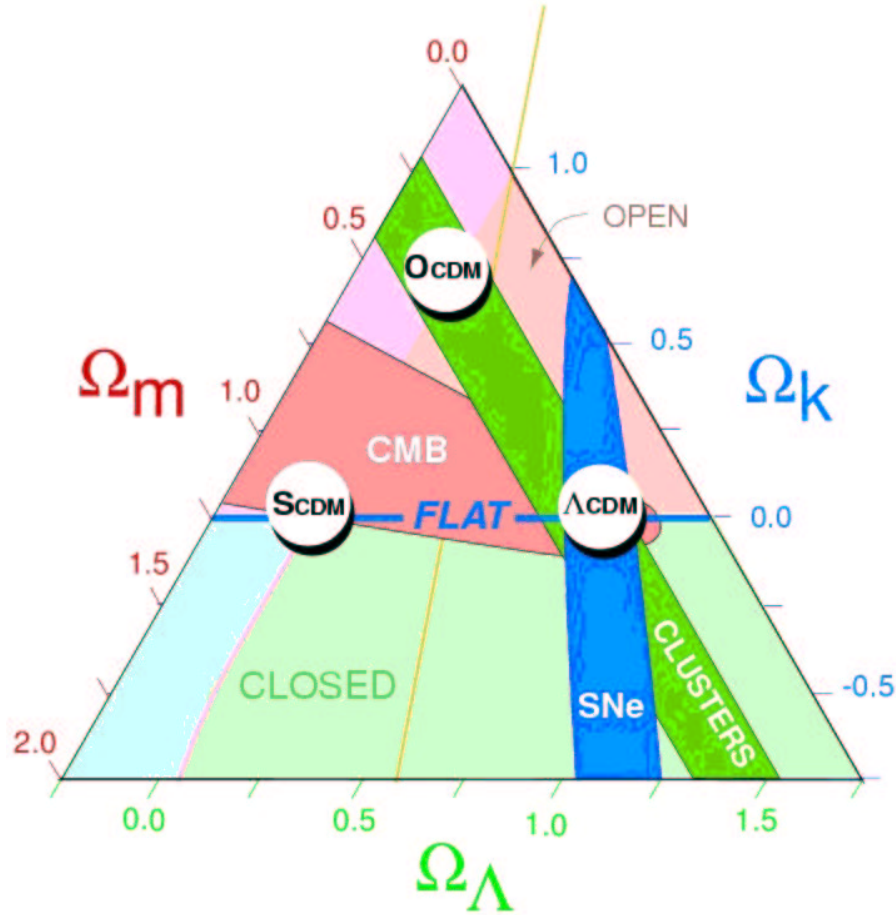


Figure 59: Fundamental triangle for cosmic density parameters.

- The cosmological microwave background (CMB) radiation tells us that the total energy density of the Universe, Ω_{tot} , is very close to the critical value marking the boundary between open and closed universes. This information is provided, in particular, by the value of the multipole $l \simeq 210$ at which the first acoustic peak appears in the CMB (Fig. 60). This tells us, in effect, the relative sizes of the Universe today and when the nuclei and free electrons in the primordial plasma combined to form neutral atoms. There are now indications for a second and even a third acoustic peak in the CMB at higher l , but these are not yet securely established. However, the magnitudes of the fluctuations $\Delta T/T$ at these larger values of l already tell us that the overall baryon density $\Omega_b \ll 1$, agreeing to within 50% with the value estimated on the basis of Big Bang nucleosynthesis calculations. Much more accurate

²Derive the energy conservation $dE + P dV = 0$ for Friedman models.

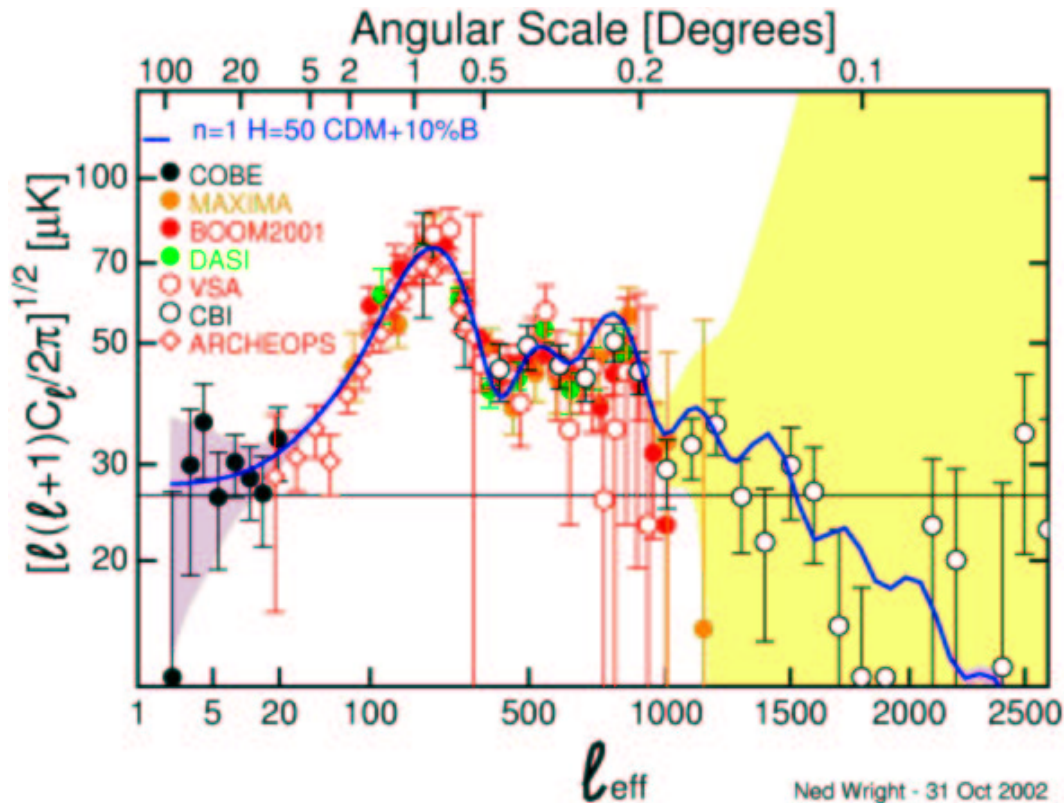


Figure 60: CMB temperature fluctuations as known in 2002. The existence of the first acoustic peak has been confirmed by balloon experiments (Boomerang and Maxima). In May 2002 two new sets of high angular resolution measurements from interferometers were announced by the Very Small Array (VSA) and the Cosmic Background Imager (CBI). The yellow band is the expected noise from the MAP mission which was launched on 30 June 2001.

results are expected from the MAP mission up to $l \simeq 1000$.

- The amount of dark matter lurking in the clusters of galaxies can easily be determined by measuring the gas distribution in the clusters (Fig. 61).³

Dark matter and elliptical galaxies: A Chandra image of NGC 720 (Fig. ??) shows a galaxy enveloped in a slightly flattened, or ellipsoidal cloud of hot gas that has an orientation different from that of the optical image of the galaxy. The flattening is too large to be explained by theories in which stars and gas are assumed to contain most of the mass in the galaxy. The temperature of the gas is 7 million degrees K.

³Discuss methods to derive the total mass in galaxy clusters.

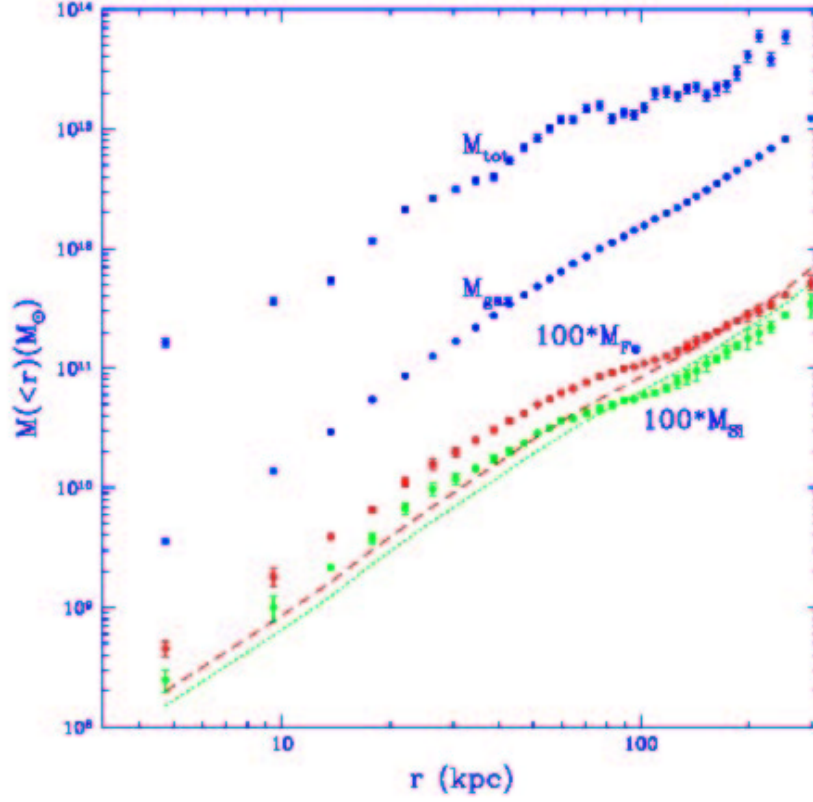


Figure 61: Mass distribution in the Hydra cluster as derived from Chandra observations. The total mass exceeds the gas mass by about a factor of 10.

According to the standard theory of gravity, the X-ray producing cloud would need an additional source of gravity – a halo of dark matter – to keep the hot gas from expanding away. The mass of dark matter required would be about five to ten times the mass of the stars in the galaxy.

Combining the CMB and high- z supernova data, one finds fairly accurate values for the cosmological density parameters (Fig. 63):

$$\Omega_{\text{tot}} = 1.02 \pm 0.06 \quad , \quad \Omega_M h^2 = 0.13 \pm 0.05 \quad (98)$$

$$\Omega_\Lambda = 0.5 \pm 0.2 \quad , \quad \Omega_B h^2 = 0.022 \pm 0.004 \quad (99)$$

The standard paradigm is that large-scale structures in the Universe are formed by gravitational instabilities, building on the primordial density perturbations observed in the CMB, with baryons falling into the ‘holes’ that are amplified by cold dark matter. Galaxy formation is considered to be more complex than cluster forma-

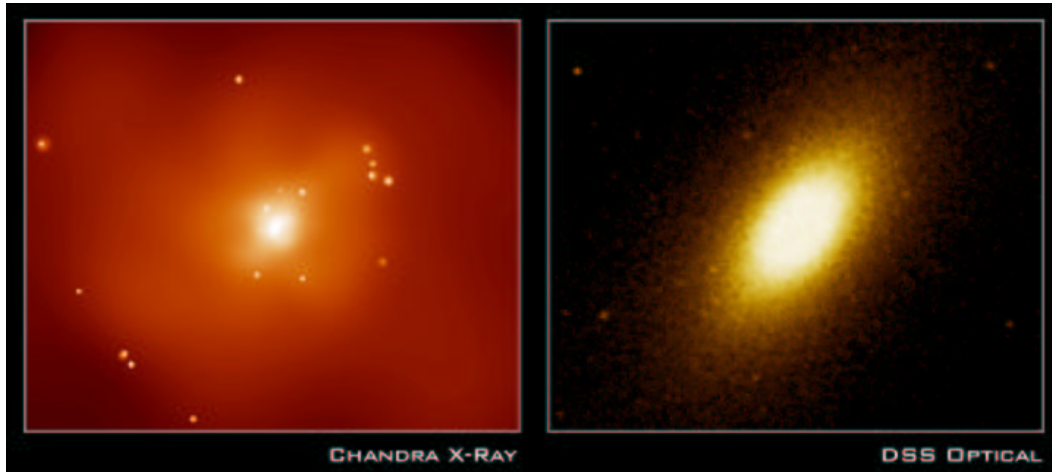


Figure 62: A Chandra image shows that the elliptical galaxy NGC 720 is embedded into a halo of dark matter. The total mass exceeds the gas mass by about a factor of 5 to 10. [Chandra observatory]

tion, with nonlinear astrophysical processes coming into play. Calculating galaxy formation is therefore more challenging numerically, though it may be guided by semi-analytical models. The general belief is that clusters formed before galaxies, which were formed by mergers of smaller structures.

On the nature of dark matter: Dark matter is probably formed by some exotic particles left over from the early Universe. The most probable candidate is the neutralino, a supersymmetric fermionic particle with mass in the range from 100 GeV to 10 TeV. These particles interact nowadays only via gravitational forces, and their cross-sections are extremely small. In distinction to baryons, dark matter behaves as a collisionless fluid. The presence of dark matter can only be observed over gravity effects, e.g. in clusters of galaxies or in rotation laws for disk galaxies. Since $\Omega_{DM} \gg \Omega_B$, the formation of structure in the late Universe is essentially dictated by dark matter. Baryons just follow the gravitational potential formed by dark matter.

On the nature of the dark energy: The observational evidence that the Universe is accelerating today changes the study of inflation from archeology to real-time ghost hunting and implies that our Universe is dominated by energy with negative pressure or that Einstein's General Relativity is incorrect on large scales. This dark energy could come from the condensation of dark matter (in the CDM framework). The idea that acceleration might be induced by a condensate has been discussed by various authors. It has been suggested that a scalar condensate might

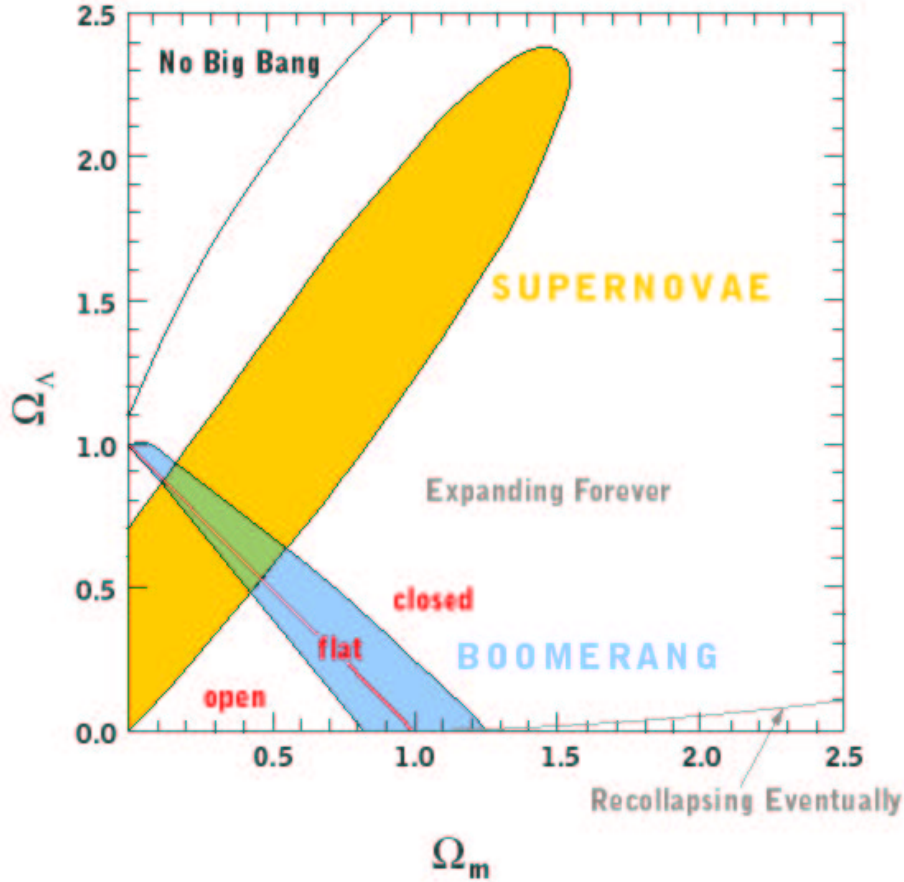


Figure 63: The fundamental plane of cosmology.

arise in an effective field theory description of gravity (Brandenberger & Zhitnitsky 1997). From condensed matter theory we are familiar with condensates forming at very low temperatures. An example is a superconductive material, where a phase transition takes place and the electrons form Cooper pairs. These Cooper pairs are collectively described by a boson field.

In our Universe, when the temperature of the Universe reaches a suitable value, the cold dark matter which could be associated with fermions (e.g. the neutralino), might undergo a phase transition where a condensate of fermion–fermion pairs would emerge (Bassett et al. 2002). Such pairs would then be described by an effective scalar field theory. Initially, cold dark matter scales as dust ($w = 0$). If after the transition, the final equation of state of the condensate $w_f < -1/3$, where $P_f = w_f \rho_f$, then the scalar field dynamics will drive the Universe into an accelerating phase. Caldi & Chodos (1999) have observed that a cosmological constant with the energy–scale $\Lambda \simeq (10^{-3} \text{ eV})^4$ could be explained by neutrino condensation.

3.5 The Present Universe is 14 Billion Years Old

Cosmic time t can be recovered from the Friedman equation

$$\begin{aligned} dt &= \frac{dt}{da} da = -\frac{dt}{da} \frac{dz}{(1+z)^2} \\ &= -\frac{1}{H_0} \frac{dz}{(1+z)^2 \sqrt{\Omega_M(1+z) + \Omega_\Lambda/(1+z)^2 + 1 - \Omega_M - \Omega_\Lambda}}, \end{aligned} \quad (100)$$

and therefore

$$t(z) = \int_0^t dt = -\frac{1}{H_0} \int_\infty^z \frac{dz'}{(1+z') \sqrt{(1+z')^2(1 + \Omega_M z') - \Omega_\Lambda z'(2+z')}}. \quad (101)$$

This formula can be integrated numerically. In the case of an inflationary Universe, $k = 0$, the above expression can be simplified

$$t(z) = \int_0^t dt = -\frac{1}{H_0} \int_\infty^z \frac{dz'}{(1+z') \sqrt{\Omega_M(1+z')^3 + \Omega_\Lambda}}. \quad (102)$$

With the transformation

$$\tan \theta(z) = \sqrt{\frac{\Omega_M}{\Omega_\Lambda}} (1+z)^{3/2} \quad (103)$$

an analytical expression can be derived

$$t(z) = \frac{2}{3H_0\sqrt{\Omega_\Lambda}} \ln \left[\frac{1 + \cos \theta(z)}{\sin \theta(z)} \right]. \quad (104)$$

Age constraints follow from observations of globular clusters, old halo stars and old White Dwarfs in the halo (Chaboyer 2002). The oldest stars are compatible with an age

$$t_0^* = (13.2 \pm 1.2) \text{ Gyrs}. \quad (105)$$

The first stars are probably formed within less than one Giga-year from the Big-Bang. An age of the Universe of 14 Giga-years is presently compatible with all observations (Fig. 64).

3.6 Observing Quasars in an Expanding Universe

Besides the redshift, which is an expression for the expansion of the Universe, $1+z = R_0/R(t)$ for given expansion factor $R(t)$, the particular form of $R(t)$ enters essentially into

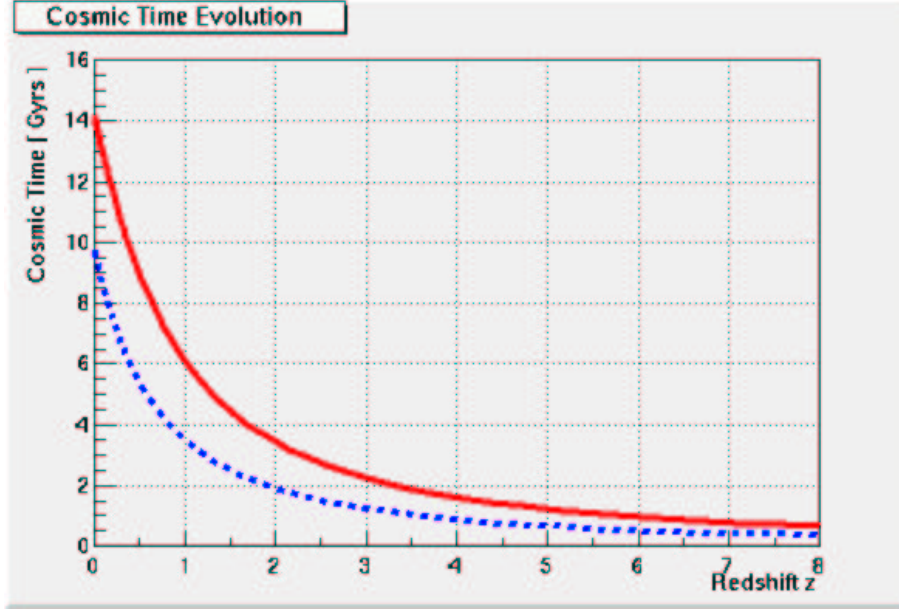


Figure 64: Age as a function of redshift for a Hubble constant $H_0 = 65$ km/Mpc/s. The lower curve corresponds to a classical Friedmann Universe without vacuum energy, the upper curve to a standard flat model with $\Omega_M = 0.3$ and $\Omega_\Lambda = 0.7$. For a quasar at redshift 6, the Universe had an age of one Giga-year, the present Universe is about 14 Giga-years old.

- **luminosity distance** $d_L(z)$ which is defined by the observed flux f_B in some wavelength filter and the corresponding intrinsic luminosity L_B

$$f_B = \frac{L_B}{4\pi d_L^2(z)}. \quad (106)$$

- **angular width** Θ of an object of dimension D (a core or jet e.g.)

$$\Theta = \frac{D}{d_A(z)} = \frac{D(1+z)^2}{d_L} \quad (107)$$

for given angular distance $d_A(z)$;

- **number counts** of objects in a redshift interval, $dN/dz d\Omega$, for given solid angle $d\Omega$ (galaxies, quasars etc.).

3.6.1 Luminosity Distance and Hubble Diagrams

Let $L dt_1$ be the total energy, emitted by a Quasar at time $t_1 < t_0$. This energy is detected by an observer in the time interval $dt_0 = dt_1 (R(t_0)/R(t_1))$ and is redshifted

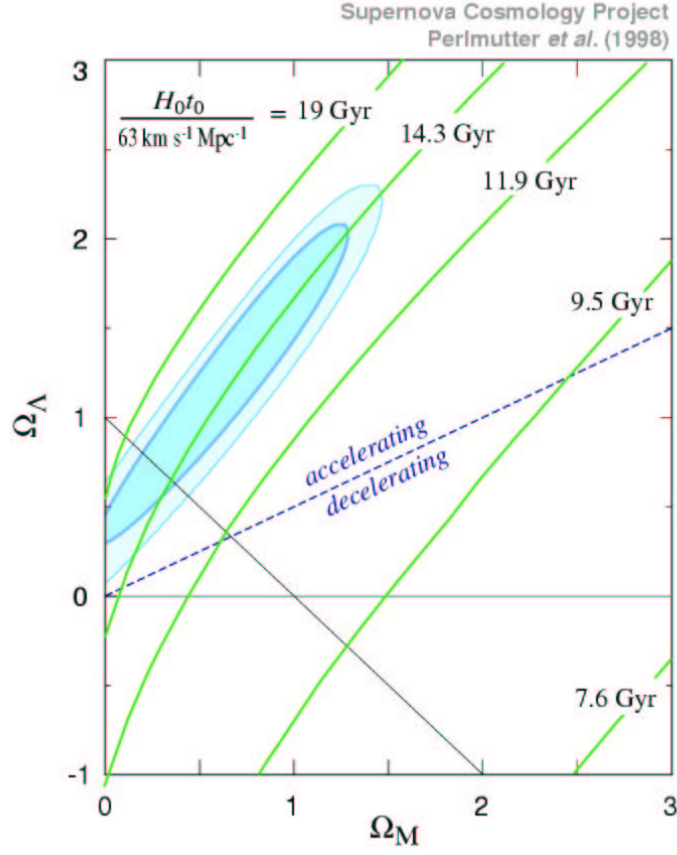


Figure 65: Age relations in the fundamental plane of cosmology. The present data are all compatible with a flat Universe of 14 billion years old. Dark matter contributes $\Omega_M = 0.3$, vacuum energy $\Omega_\Lambda = 0.7$

by the factor $R(t_1)/R(t_0)$. For $t = \text{const}$ and $r = \text{const}$ we have the line element for a sphere

$$ds^2 = -r^2 R^2 (d\theta^2 + \sin^2 \theta d\phi^2). \quad (108)$$

The light emitted by the Quasar is distributed over a sphere with surface $A = 4\pi r^2 R^2(t_0)$ at time t_0 . The flux detected in dt_0 is therefore given by

$$F dt_0 = L dt_1 \frac{R(t_1)}{R(t_0)} \frac{1}{4\pi R^2(t_0) r_1^2} = \frac{L}{4\pi R_0^2 r_1^2} \left(\frac{R(t_1)}{R(t_0)} \right)^2. \quad (109)$$

This determines the bolometric flux

$$F_{\text{bol}} = \frac{L}{4\pi r_1^2 R^2(t_0) (1+z)^2} = \frac{L}{4\pi d_L^2} \quad (110)$$

For this reason, the distance

$$\boxed{d_L = r_1 R(t_0)(1+z)} \quad (111)$$

is known as the **luminosity distance** of a Quasar with redshift z . The distance modulus is a fundamental quantity for quasars

$$m(z) - M = 5 \log d_L(z; H_0, \Omega_M, \Omega_\Lambda) + 25, \quad (112)$$

which relates the apparent magnitude $m(z)$ with the absolute magnitude M for a Quasar at distance d_L [Mpc]. This is calculated from $d_L(z) = r_1 R_0(1+z)$, where r_1 is the solution of the equation

$$R_0 \int_0^{r_1} \frac{dr}{\sqrt{1-kr^2}} = R_0 \int_{t_1}^{t_0} \frac{c dt}{R(t)}. \quad (113)$$

With the formal solution of the Friedman equation (94) this can be written as

$$R_0 \int_0^{r_1} \frac{dr}{\sqrt{1-kr^2}} = \frac{c}{H_0} \int_{t_1}^{t_0} \frac{da}{a \sqrt{\Omega_M/a + \Omega_\Lambda a^2 + 1 - \Omega_M - \Omega_\Lambda}}. \quad (114)$$

Since $da = -dz/(1+z)^2$, one obtains

$$\frac{R_0 dr}{\sqrt{1-kr^2}} = -\frac{c}{H_0} \frac{dz}{E(z)} \quad (115)$$

with

$$E(z) \equiv \sqrt{\Omega_k(1+z)^2 + \Omega_M(1+z)^3 + \Omega_\Lambda} \quad (116)$$

and $E(0) = 1$. This provides us the solution for the luminosity distance

$$d_L(z; H_0, \Omega_M, \Omega_\Lambda) = \frac{c(1+z)}{H_0 \sqrt{|\Omega_k|}} \mathcal{S}(x[z]), \quad (117)$$

where

$$x[z] = \sqrt{|\Omega_k|} \int_0^z \frac{dz'}{\sqrt{(1+z')^2(1+\Omega_M z') - z'(2+z')\Omega_\Lambda}}. \quad (118)$$

$\mathcal{S}(x)$ denotes the functions $\sinh(x)$, x oder $\sin(x)$ depending on the curvature of space, i.e. for $\Omega_k > 0$, $\Omega_k = 0$ or $\Omega_k < 0$, respectively. For a flat Universe (Λ CDM), we obtain simply

$$d_L(z; H_0, \Omega_M) = \frac{c(1+z)}{H_0} \int_0^z \frac{dz'}{\sqrt{\Omega_M(1+z')^3 + 1 - \Omega_M}}. \quad (119)$$

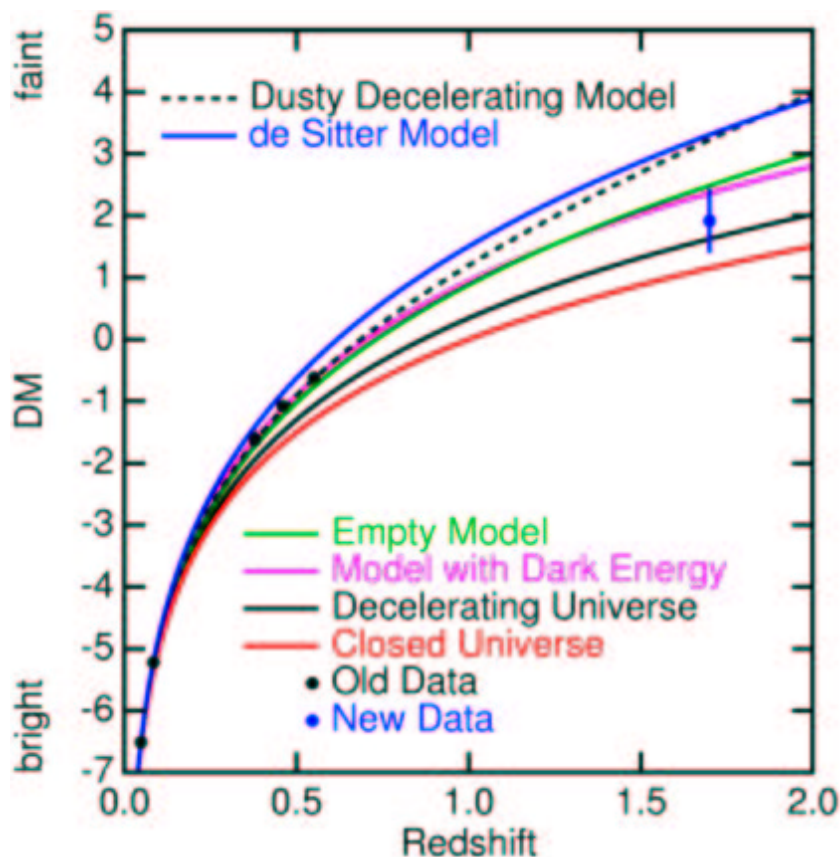


Figure 66: Distance modulus $DM = m - M$ of the luminosity distance as a function of redshift. The de Sitter Universe, which is dominated by vacuum energy, acts as an attractor for all other solutions. For high-redshift quasars differences up to two magnitudes are obtained.

Besides the overall scaling of distances by

$$\frac{c}{H_0} = 4615 \text{ Mpc} \frac{65 \text{ km/Mpc/s}}{H_0} \quad (120)$$

the luminosity distance merely depends on the density parameter. This has as a limit the famous luminosity distance in a flat classical Friedmann Universe (SCDM), $\Omega_\Lambda = 0$,

$$d_L(z; H_0) = \frac{2c}{H_0} \left[1 + z - \sqrt{1 + z} \right]. \quad (121)$$

It is then easily shown that the Hubble-law $d_L \simeq cz/H_0$ follows in the limit $z \ll 1$, typically valid for redshifts $z < 0.1$. This is the flat space-limit of the famous Mattig

formula (Mattig 1958) for models with $\Omega_\Lambda = 0$, $q_0 = \Omega_M/2$,

$$d_L(z; q_0) = \frac{c}{H_0} \frac{1}{q_0^2} \left[q_0 z - (1 - q_0)(1 - \sqrt{1 + 2q_0 z}) \right]. \quad (122)$$

For general models with non-vanishing cosmological constant, the integrals have to be done numerically (Fig. 66).

3.6.2 The Angular Width

The angular width of an object can easily be calculated for standard models with the luminosity distance (121). This function has a minimum, which is easily calculated (SCDM model)

$$\Theta(z) = \frac{DH_0}{2c} \frac{(1+z)^{3/2}}{\sqrt{1+z-1}}. \quad (123)$$

The minimum is achieved at a redshift

$$z_{\min} = 1.25 \quad (124)$$

and the minimal angular width of an object with intrinsic dimension D is given by⁴

$$\Theta_{\min} = 3.375 \frac{DH_0}{c} = 0.12 (2h) \text{ mas} \left(\frac{D}{\text{pc}} \right). \quad (125)$$

1 mas = 1 milli-arcsecond. The width of the core of M 87 at a redshift of 1.25 would be about 0.16 arcsec, i.e. just resolvable with HST. Normal galaxies appear in fact on the Hubble deep field with dimensions of a few arcsec. Without this focussing effect of the expanding Universe, objects beyond redshift one would appear pointlike. Also the jets of quasars and radio galaxies are not becoming smaller at high redshifts.

3.6.3 Number Counts

Let us assume that we have at time t_1 $n(t_1; L) dL$ quasars per unit volume having an absolute luminosity between L and $L + dL$. The total number of these objects on the whole Sky is then given by

$$dN = 4\pi \frac{R(t_1) dr_1}{\sqrt{1 - kr_1^2}} R^2(t_1) r_1^2 n(t_1; L) dL. \quad (126)$$

With $r_1 = r(t_1)$ and the light cone condition

$$dr_1 = -\sqrt{1 - kr_1^2} \frac{c dt_1}{R(t_1)} \quad (127)$$

⁴ $DH_0/c = 0.44 (D/10 \text{ kpc})$ for $h = 0.65$

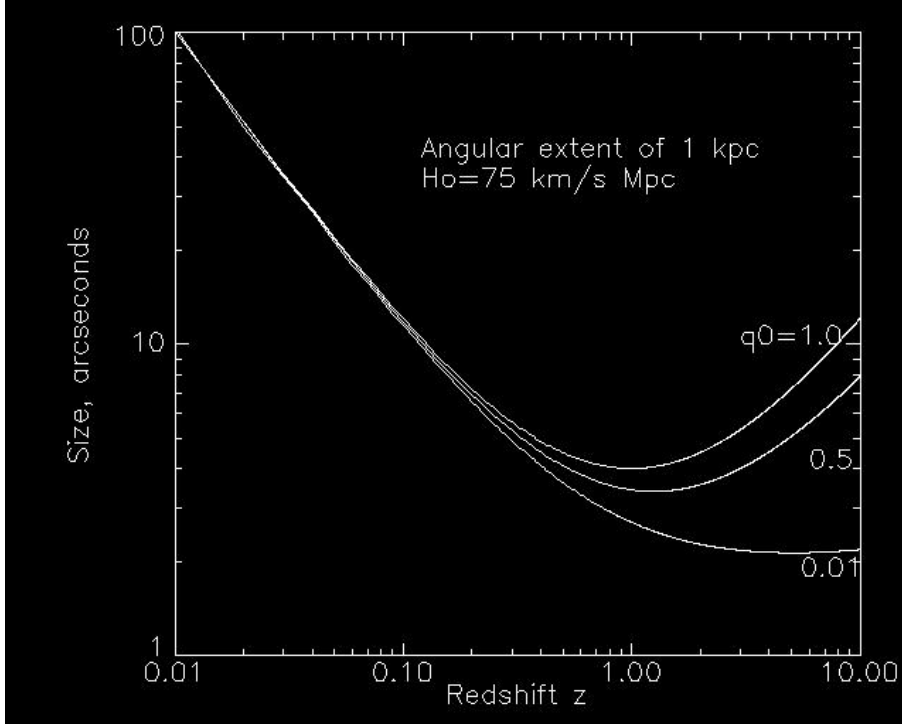


Figure 67: Apparent angular width for an elliptical galaxy of 10 kpc extension, parametrised by q_0 in a Universe without vacuum energy. The angular width attains a minimum at redshift $z \simeq 1.2$.

we get

$$dN = 4\pi R^2(t_1) r_1^2 n(t_1; L) c |dt_1| dL. \quad (128)$$

Using the relation between redshift and time, given by the Friedman-equation

$$dt = -\frac{1}{H_0} \frac{dz}{(1+z)E(z)} \quad (129)$$

we then find, $d_H = c/H_0$,

$$dN = 4\pi d_H R^2(t_0) r_1^2 n(z_1; L) \frac{dz dL}{(1+z)^3 E(z)}. \quad (130)$$

This can be expressed in terms of the luminosity distance, $d_L = r_1 R_0 (1+z)$,

$$dN(z; L) = 4\pi d_H \frac{d_L^2(z)}{(1+z)^5 E(z)} n(z; L) dz dL. \quad (131)$$

For $z < 0.1$ we have

$$dN(z; L) \simeq 4\pi d_H^3 z^2 n(z; L) dz dL. \quad (132)$$

For the classical Friedman models (SCDM) ($\Omega_\Lambda = 0$) one finds

$$dN(z; L) = 4\pi d_H \frac{d_L^2}{(1+z)^6 \sqrt{1+\Omega z}} n(z; L) dz dL. \quad (133)$$

If the total number of objects is conserved

$$n(z; L) = n(0; L) (1+z)^3, \quad (134)$$

the redshift distribution for objects brighter than the apparent magnitude m is given by

$$dN(z; < m) = 4\pi d_H \int_0^\infty dL \frac{d_L^2}{(1+z)^2 E(z)} n(0; L) dz. \quad (135)$$

If there were a class of objects in the Universe with constant luminosity (e.g. SN Ia), the redshift distribution of such objects were simply given by

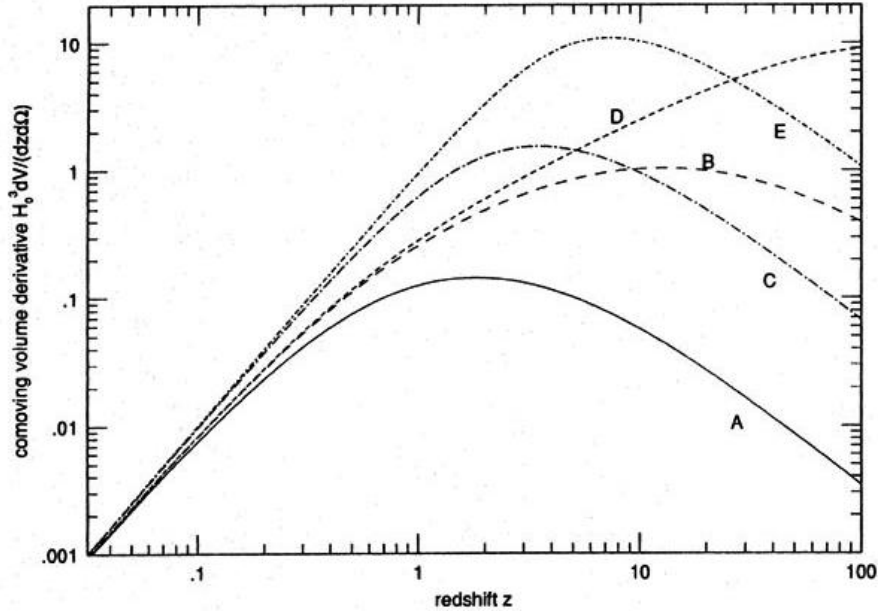


Figure 68: Comoving cosmic volume per redshift interval dz and per steradian as a function of redshift for various models (normalized in the Hubble-volume d_H^3): A: $k = 0$, $\Omega_M = 1$ (SCDM); B: $k = -1$, $\Omega_M = 0.1$, $\Omega_\Lambda = 0$ (open); C: $k = 0$, $\Omega_M = 0.1$, $\Omega_\Lambda = 0.9$ (Λ CDM); D: $k = 0$, $\Omega_M = 0$, $\Omega_\Lambda = 1$ (de Sitter); E: $k = 0$, $\Omega_M = 0.01$, $\Omega_\Lambda = 0.99$ (fast de Sitter). In a Λ CDM-model, this volume attains a maximum at a redshift $z \simeq 2$ and decays afterwards with $(1+z)^{-3/2}$. In a de Sitter Universe this volume would converge towards a constant value.

$$dN(z) = 4\pi d_H n(0) \frac{d_L^2(z)}{(1+z)^2 E(z)} dz. \quad (136)$$

The volume

$$dV_C(z) = d_H \frac{d_L^2(z)}{(1+z)^2 E(z)} d\Omega dz \quad (137)$$

is usually denoted as **comoving volume**. This differential volume element depends critically on the particular cosmological model (Fig. 68). Could we observe SNe up to redshift of 5, so we could in principle derive the cosmological model. This function has its maximum at a redshift of 2. For galaxies and Quasars, this redshift distribution is however much more complicated, since it has to be convolved with the luminosity function. In addition, galaxies and Quasars are observed only up to some limiting magnitude. This fact leads to an exponential cutoff in the observed redshift distribution (Fig. 69), since at high redshifts only the most luminous objects can be observed. Since Quasars are up to 5 magnitudes brighter than galaxies, they can be observed to high redshifts. It is interesting that Quasars have a redshift distribution with its maximum around 2. The decay beyond 2 is probably dictated by number evolution, there are simply less objects with extremely high redshifts, the number density is not conserved.

All astronomical objects follow some complicated **luminosity function** $\Phi(L) dL$ which has typically a cutoff at high luminosities. The Schechter-function

$$\Phi(L) dL = \Phi_0 (L/L_*)^{-\alpha} \exp(-L/L_*) \quad (138)$$

is a classical example for the representation of the galaxy distribution. In this case, the integral in (135) can be done numerically. The conversion of absolute luminosity into observed flux adds another factor z^2 for the low-redshift behaviour, so that $dN(z; < m)/dz \propto z^4$ for $z \ll 1$. At higher redshifts, the exponential cutoff leads to a rapid decay in the number distribution. This is well observed e.g. in the redshift distribution of galaxy surveys.

3.6.4 The K-Correction

We consider a quasar (or galaxy) observed at redshift z . The apparent flux of the source is measured through a finite observer-determined bandpass R and the intrinsic luminosity is measured through a finite emitter-defined bandpass Q . The K-correction tries to relate these two quantities.

Consider a quasar to have apparent magnitude m_R when observed through a photometric bandpass R . M_Q denotes then the absolute magnitude defined in the emitter bandpass Q . The K-correction K_{QR} is defined as

$$m_R = M_Q + DM + K_{QR}, \quad (139)$$

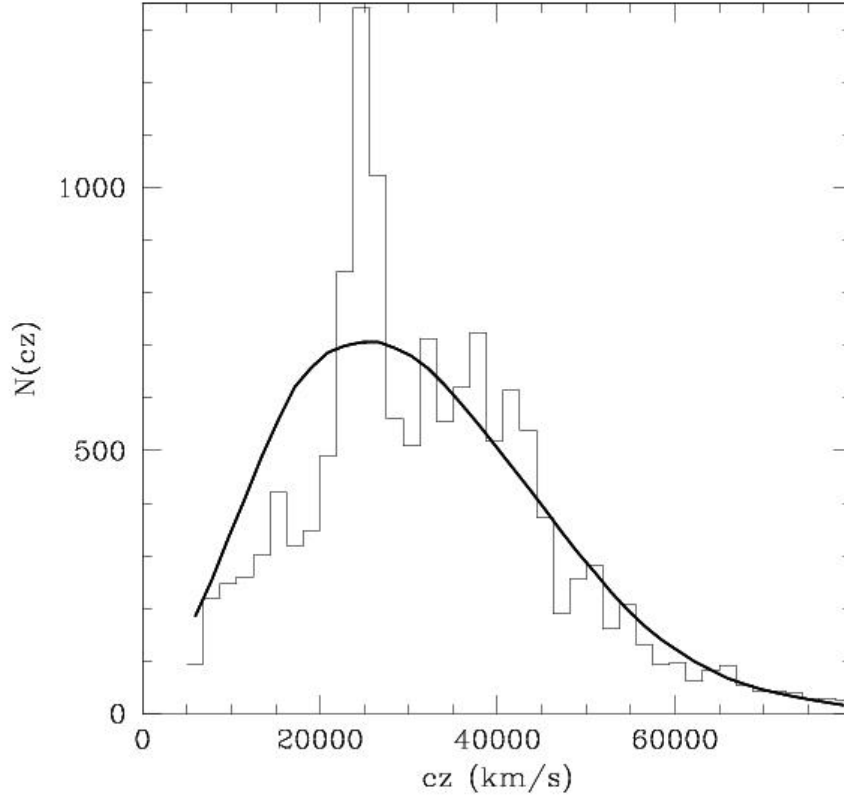


Figure 69: Number distribution for galaxies observed in SDSS and compared to a given luminosity function with exponential cutoff. The maximum occurs at a redshift of about 0.1.

where DM is the distance–module defined as

$$DM = 5 \log \left(\frac{d_L}{10 \text{ pc}} \right). \quad (140)$$

The apparent magnitude m_R of the quasar is related to the spectral flux

$$m_R = -2.5 \log \left[\frac{\int d \ln \nu_0 f_\nu(\nu_0) R(\nu_0)}{\int d \ln \nu_0 g_\nu^R(\nu_0) R(\nu_0)} \right], \quad (141)$$

where the integrals are over the observed frequencies. $g_\nu^R(\nu)$ is the spectral density of flux for the zero–magnitude source (magnitude calibration, Vega–like A0 stars). For AB–magnitudes, this is a hypothetical constant source with $g_\nu^{AB}(\nu) = 3631 \text{ Jy}$ at all frequencies. $R(\nu)$ describes the bandpass of the detector.

The absolute magnitude M_Q is defined to be the apparent magnitude that the quasar would have at a distance of 10 pc. It is related to the spectral luminosity density L_ν (energy per unit time per unit frequency)

$$M_Q = -2.5 \log \left[\frac{\int d \ln \nu_e (L_\nu(\nu_e)/4\pi[10 \text{ pc}]^2) Q(\nu_e)}{\int d \ln \nu_e g_\nu^Q(\nu_e) Q(\nu_e)} \right], \quad (142)$$

where the integrals are now over emitted frequencies, and $Q(\nu)$ is the equivalent of $R(\nu)$, but for the bandpass Q .

If the quasar is at redshift z , then its luminosity is given by

$$L_\nu(\nu_e) = \frac{4\pi d_L^2(z)}{1+z} f_\nu(\nu_0) \quad (143)$$

and $\nu_e = (1+z)\nu_0$. The factor $1+z$ accounts for the fact that the flux and luminosity are not bolometric, but densities per unit frequency.

Equation (141) holds if the K-correction is given by

$$K_{QR} = -2.5 \log \left[(1+z) \frac{\int d \ln \nu_0 f_\nu(\nu_0) R(\nu_0) \int d \ln \nu_e g_\nu^Q(\nu_e) Q(\nu_e)}{\int d \ln \nu_0 g_\nu^R(\nu_0) R(\nu_0) \int d \ln \nu_e f_\nu(\nu_e/(1+z)) Q(\nu_e)} \right], \quad (144)$$

The K-correction is here defined in terms of the observed flux. This is the direct observable. The transformation from the observed flux to the emitted luminosity gives the following expression for the K-correction

$$K_{QR} = -2.5 \log \left[(1+z) \frac{\int d \ln \nu_0 L_\nu(\nu_0(1+z)) R(\nu_0) \int d \ln \nu_e g_\nu^Q(\nu_e) Q(\nu_e)}{\int d \ln \nu_0 g_\nu^R(\nu_0) R(\nu_0) \int d \ln \nu_e L_\nu(\nu_e) Q(\nu_e)} \right], \quad (145)$$

In all these calculations frequency is used. In terms of wavelengths one considers the relation $\nu f_\nu(\nu) = \lambda f_\lambda(\lambda)$, $\lambda\nu = c$. The K-correction then becomes

$$K_{QR} = -2.5 \log \left[\frac{1}{1+z} \frac{\int \lambda_0 d\lambda_0 f_\lambda(\lambda_0) R(\lambda_0) \int \lambda_e d\lambda_e g_\lambda^Q(\lambda_e) Q(\lambda_e)}{\int \lambda_0 d\lambda_0 g_\lambda^R(\lambda_0) R(\lambda_0) \int \lambda_e d\lambda_e f_\lambda((1+z)\lambda_e) Q(\lambda_e)} \right], \quad (146)$$

A transformation from observed flux f_λ to emitted-frame luminosity $L_\lambda(\lambda_e)$ gives

$$K_{QR} = -2.5 \log \left[\frac{1}{1+z} \frac{\int \lambda_0 d\lambda_0 L_\lambda(\lambda_0/(1+z)) R(\lambda_0) \int \lambda_e d\lambda_e g_\lambda^Q(\lambda_e) Q(\lambda_e)}{\int \lambda_0 d\lambda_0 g_\lambda^R(\lambda_0) R(\lambda_0) \int \lambda_e d\lambda_e L_\lambda(\lambda_e) Q(\lambda_e)} \right], \quad (147)$$

This equation becomes identical to the equation given in Oke & Sandage (1968) and Kim et al. (1996), if it is assumed that $Q = R$, i.e. $g_\nu^Q = g_\nu^R$. Some variables have also to be transformed: $\lambda_0 = \lambda_e$, $F(\lambda) = L_\lambda$ and $S_i(\lambda) = \lambda R(\lambda)$.

To compute an accurate K-correction, one needs an accurate description of the source flux f_ν , the standard source flux densities g_ν^R and g_ν^Q , and the bandpass functions $R(\nu)$ and $Q(\nu)$. In real astronomical situations, these are typically known only within a few percent accuracy. The classical K-correction has $Q = R$. This eliminates the integrals over the standard source flux densities g_ν^R .

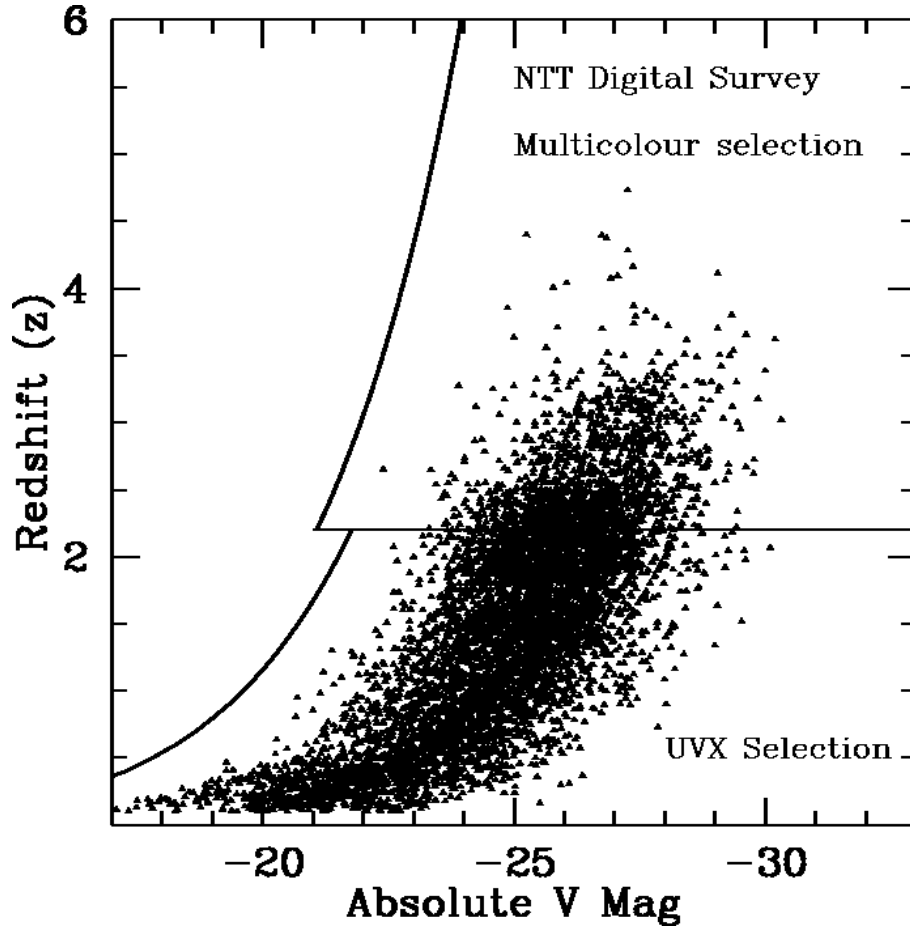


Figure 70: Luminosity evolution of Quasars with redshift.

3.7 Luminosity Evolution of Quasars

Fig. 71 shows the optical luminosity function (OLF) for ten separate data subsets divided by redshift from the 2dF redshift survey. The evolution as a function of redshift is obvious and over the redshift range $0.35 < z < 2.3$ is acceptably fit by pure luminosity evolution (PLE). That is, the form of the OLF does not vary with redshift, but is simply shifted to higher luminosity. The shape and evolution at low redshifts ($z < 0.5$) and high luminosities are not currently well sampled by the 2QZ, but may show departures from PLE. This issue will be addressed in more detail with the complete 2QZ catalogue, supplemented with the FLAIR/6dF QSO survey and similar surveys (SDSS etc).

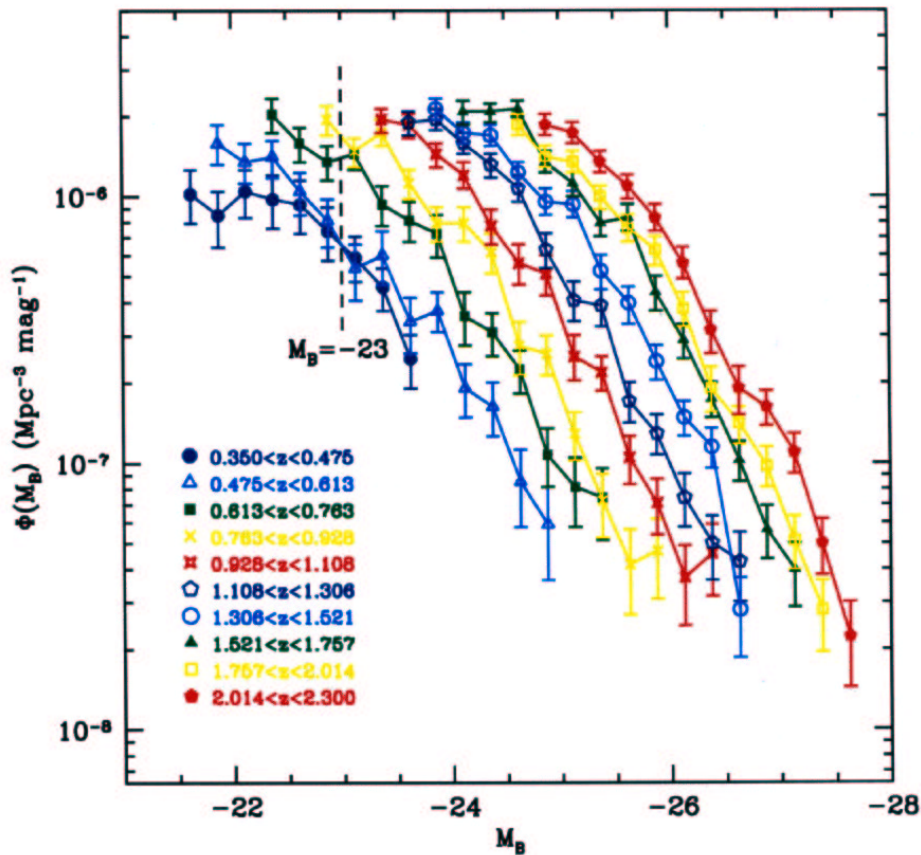


Figure 71: Luminosity function of Quasars as obtained from the 2dF survey, sampled into 10 redshift bins.

3.8 Cosmology with Quasars

Quasars at high redshifts can be used to study the universe early in its history, and absorption features from intervening objects can yield information about conditions subsequent to the time when the quasar emitted its light in our direction. Furthermore the spatial and luminosity distribution functions of these high- z quasars can shed light on the formation of structure in the early universe. The Sloan Digital Sky Survey (SDSS) has the potential to identify more of these objects than any survey to date, and thus provide an unprecedented sample for followup study.

Because high-redshift quasars are receding at relativistic velocities the Lyman alpha emission line is shifted from the ultraviolet into the red region of the electromagnetic spectrum. The Next Generation Space Telescope (NGST) will be optimized in the infrared in order to detect very distant objects at redshifts greater than

$z = 5$. The properties of the intergalactic medium can be studied back to the time of galaxy formation using distant quasars. The number density of absorption lines as a function of epoch will provide an important cosmological test. Observations of correlated absorption, both in redshift and in nearby quasars on the plane of the sky, are leading to important information on the evolution of the large-scale distribution of galaxies in space. The Lyman alpha clouds offer the opportunity to investigate the evolution of the intergalactic medium and the meta-galactic ionizing radiation flux and to provide information on primordial abundances of the elements.

References

- [1] Bassett, B.A. et al. 2002, astro-ph/0211303
- [2] Chaboyer, 2002, Moriond Lectures
- [3] Freedman, W. et al. 2001, ApJ 553, 47
- [4] Kim, A. Goobar, A., Perlmutter, S. 1996, PASP 190–201
- [5] Mattig, W. 1958, Astron. Nachr. 284, 109.
- [6] Oke, J.B., Sandage, A. 1968, ApJ 154, 21
- [7] Peebles, P.J.E., Ratra, B. 2002, “The Cosmological Constant and Dark Energy”, astro-ph/0207347.
- [8] Perlmutter, S. et al. 1998, Nature 391
- [9] Perlmutter, S. et al. 1999, ApJ 517, 566
- [10] Riess, A.G., Press, W.H., Kirshner, R.P. 1996, ApJ 473, 88.